Richard P. Woodward and Joseph R. Dolonski
Lewis Research Center
Cleveland, Ohio

Prepared for the
Eighth Aeroacoustics Conference
sponsored by the American Institute of Aeronautics and Astronautics
Atlanta, Georgia, April 11-13, 1983

NASA

TONE GENERATION BY ROTOR-DOWNSTREAM STRUT INTERACTION

Richard P. Woodward and Joseph R. Balombin

National Aeronautics and Space Administration
Lewis Research Center
Cleveland, Ohio 44135

Abstract

A JT15D fan stage was acoustically tested in the NASA Lewis anechoic chamber as part of the joint Lewis-Langley Research Center investigation of flight simulation techniques and flight effects using the JT15D engine as a common test vehicle. Suspected rotor-downstream support strut interaction was confirmed through the use of simulated support struts which were tested at three axial rotor-strut spacings. Tests were also performed with the struts removed. Inlet boundary layer suction in conjunction with an inflow control device was also explored. The removal of the boundary layer reduced the fan fundamental tone levels suggesting that the mounting and mating of such a device to the nacelle requires careful attention. With the same inflow control device installed good acoustic agreement was shown between the engine on an outdoor test stand and the fan in the anechoic chamber.

Introduction

The development of effective inflow control devices (ICD's) makes it possible to study noise generation mechanisms, such as rotor-stator interaction, with reduced masking effects of inflow disturbances. Modern turbofan engines are often designed with blade/vane numbers selected to prevent propagation of the fundamental rotor-stator interaction tone. However, less consideration has been given to possible rotor interactions with engine support struts. These struts are either located downstream of the stator row or are integrated into the stator as large cross-section vanes.[1]

This paper presents for a JT15D fan stage which was acoustically tested in the NASA Lewis Research Center anechoic chamber[2] as part of a joint NASA Lewis-Langley investigation of flight simulation techniques and flight effects using the JT15D-1 engine as a common test vehicle.[3-7] The engines used in these studies were instrumented with blade and vane pressure transducers to assist in isolating noise generation mechanisms. Although the primary goal of this study was to evaluate inflow control techniques, the results revealed that, for the JT15D-1 engine, in particular speed ranges the fundamental tone was controlled by the presence of six engine support struts located downstream of the stator. Blade pressure results showing a strong six per revolution disturbance pointed to these struts as the probable noise source. The interaction between the 28-blade rotor of the JT15D and the six support struts would result in a $m = 22$ acoustic spinning mode having 22 circumferential lobes. This mode was shown to exist in the inlet duct of a JT15D engine using the results from two pressure sensors located in the duct so as to allow spinning mode identification by signal phase relationship.[3] However, it was not possible to alter the support struts in the engine to establish the behavior of this apparent noise source.

Downstream support struts were not required for the JT15D fan installation in the anechoic chamber. Six simulated support struts were fabricated and installed in the test fan stage to simulate the actual engine support strut installation. These simulated struts were located at three axial spacings from the stator trailing edge. Thus, in the present study results were obtained for the spacing effect of downstream support struts as well as for fan stage alone with no downstream struts.

Two possible mechanisms could produce rotor-strut noise: the rotor wake could impinge on the struts, or the strut potential field could extend upstream to influence the rotor. Results from reference 8 suggest that this second mechanism may be the case. In this reference, tests with a two stage fan with downstream struts showed that the potential field of these struts could induce significant blade vibration in the upstream rotor. In fact, the data analysis in this reference suggests that the strut potential field is transmitted through the stator row with little loss in magnitude, resulting in an effective closer rotor-strut spacing.

The inflow control study of the JT15D fan stage in the anechoic chamber made use of two inflow control devices which were previously tested at Lewis on the JT15D-1 engine.[3,7] In addition, the anechoic chamber installation had provisions for inlet boundary layer suction. The fan stage could be run with either a hard inlet duct surface, or with a porous metal section in the outer duct wall which was connected to a suction system to allow removal of about 10 percent of the inlet airflow. Removing the boundary layer could possibly eliminate irregularities contained in streamlines near the wall before they reached the rotor, thus reducing this possible noise source. The inlet was run with hard walls except for the boundary layer suction tests. Results for another fan tested in an anechoic chamber suggested that boundary layer suction may lower the fan blade passage tone level through the removal of such flow irregularities.[9]

Apparatus and Procedure

Anechoic Chamber

Figure 1 is a photograph of the Lewis anechoic chamber. The research fan shown in the chamber does not have an inflow control device installed. Also seen in this photograph are some of the fixed-position microphones and the traversing boom microphone. Calibration of the chamber showed it to be anechoic to within 2 dB for frequencies above 200 Hz.

Research Fan

The JT15D fan stage was installed in the anechoic chamber with an ICD attached to the inlet as shown in figure 2. The fan stage used the same

bypass flow passage contours as did the actual JT15D-1 engine. The core drive of the engine was replaced by an external electric drive, with the fan airflow exhausting through a collector assembly. Table I presents selected fan stage design parameters. The production JT15D-1 engine had 33 core stator vanes. For acoustic cut-off considerations, an aerodynamically similar 71-vane core stator was used for this acoustic program. Simulated engine support struts could be installed in the fan bypass duct as shown in figure 3 at axial spacings of 2.5, 5.1 (engine design spacing), and 8.9 cm from the stator trailing edge. These struts had an axial length of 14.5 cm. The fan installation also had eight thin sheet metal turning vanes located in the core flow passage to straighten to axial the 25° flow swirl exiting the core stator. These thin cross-section vanes were not expected to affect the fan acoustic performance.

The boundary layer suction assembly shown in figure 2 allowed removal of a portion of the inlet flow near the outer wall to reduce flow irregularities in this region and hence reduce this possible noise source. Outer wall airflow was removed through a 5.4 cm (2.5 in.) length of porous treatment located 15.2 cm (6 in.) upstream of the rotor face. The inlet was run with hard walls except for the boundary layer suction tests.

Figure 2 shows the fan stage installed in the anechoic chamber with inflow control device No. 12 attached in the fan inlet. Construction details of this ICD are shown in figure 4. This ICD was shaped so that the honeycomb cells are aligned with the flow streamlines calculated from a potential flow program. A second, ICD, designated No. 5 was dimensionally similar, except that it had six rather than nine support ribs, an inner support wire mesh, and mounted on the fan inlet slightly ahead of where ICD 12 mounted. Further construction details of ICD 12 may be found in reference 7; details of ICD 5 are in reference 3. Except where noted, all results in this paper are for ICD 12.

Dynamic Instrumentation Data Reduction

In this test program, both rotor and stator were instrumented with high response pressure transducers.[10] Signals from the stator were brought out directly, while those from the rotor were FM transmitted from an antenna mounted in the spinner to another mounted along the inside casing. Results for the B3 transducer, which was located near the rotor tip (fig. 5), are presented in this paper. Installation of these small (1.2 mm diameter sensing area, 0.8 mm thickness) devices involved cementing them to shims at the blade surface, and then fairing over them.

Data reduction of the pressure signals consisted primarily of computing the average pressure over a revolution and the corresponding spectra. Spectra were computed with a nominal 20 Hz resolution, for 512 revolutions of the fan. A tachometer pulse occurring once/revolution was used to synchornize these analyses with the fan speed, so that pressure variations not synchronized to the fan speed would be discounted.

Acoustic Instrumentation

Far field acoustic data were acquired on a 7.6 m (25 ft) radius from 0° to 90° from the fan inlet axis in 10° increments. Signals from the 0.64 cm (0.25 in.) diameter microphones were recorded on magnetic tape for later narrow bandwidth spectral analysis. The output of this narrow bandwidth sound pressure level analysis was digitized and transmitted to a computer for further analysis. Using a computer reduction program, narrow bandwidth sound power level spectra were generated for the forward hemisphere (0° to 90° from the fan inlet axis).

The boom micrphone (seen in fig. 2) was used to obtain continuous directivity results at a 6.1 m (20 ft) radius centered in the plane of the fan inlet highlight. A narrow bandwidth spectral analyzer was used to determine the fundamental and overtone levels for these boom traverses.

Results and Dicussion

Aerodynamic Results

The fan operating map (fig. 6) shows the aerodynamic performance of the JT15D fan as tested in the anechoic chamber. The flow restrictions in the exhaust ducts were adjusted for fan operation on the same operating line as was measured for the JT15D-1 engine at the Lewis vertical lift facility (VLF). Overlaid results from the statically tested VLF engine tests show good agreement with the fan results.

Support Strut Effect

Since engine support struts are not needed in this anechoic chamber fan installation, an opportunity was available to perform tests both without struts and with simulated struts to better understand the apparent rotor-strut interaction observed in the engine tests. Simulated engine support struts were installed in the downstream bypass flow passage at three axial rotor-strut spacings as shown in figure 3.

Far field acoustic effects. Figure 7 shows how the sound power level (0° to 90° from the fan inlet axis) at the blade passage tone (BPT) changes with fan speed for the three strut positions and also for no struts. The struts clearly increase the tone level at the 2.5 and 5.1 cm spacings. The closest spacing results in an increase of the tone level of 10 dB at 11 300 rpm fan speed. With the struts at the engine design spacing of 5.1 cm there is still a significant strut-induced tone, with the greatest effect seen for fan operation at 11 300 rpm. There was no significant strut effect on sound power of this BPT at the 8.9 cm spacing.

The sound power level spectra for no struts and for the struts at the two closer spacings are shown in figure 8 at 11 300 rpm. Again, the strong effect of strut location on the fundamental tone can be seen. The presence of the struts has little influence on the overtone (2 x BPF and 3 x BPF) or on broadband noise levels. The spectral spike located at about 800 Hz is only seen when the struts are in place. This spike is most

inlet radiation (ref. 14) show that the effect of thickening the inlet lip (i.e., increasing the lip radius) is to move the directivity pattern forward. A thick-lipped inlet results in acoustic shielding, with less noise propagating to the aft angles. The thick-lipped inlet used for the engine tests of reference 3 is compared to that used for the fan in the anechoic chamber in figure 11. These lip curvature effects account for a directivity shift in the engine results and the apparent agreement with the lobe peak prediction of equation (2). Equation (3) in which the group velocity remains unchanged, appears to be the preferred radiation prediction, but lip shape must also be considered.

Figure 12 presents the first and second overtone directivities at 11 300 rpm. There is a small level increase at forward angles for the first overtone (fig. 10(a)) at the closest strut spacing, but no significant strut effects on the second overtone directivity (fig. 10(b)).

Blade pressure effects. The blade pressure transducer results for the fan tests also showed evidence of strut interaction. Figure 13 shows the average blade pressure at 12 000 rpm as a function of angular position for the three strut spacings and for the struts removed. With no struts and at the farthest strut spacing (figs. 13(a) and (b)) there is no observable strut effect, although there is evidence of interaction with the 66 bypass stator vanes. However, at the engine strut spacing (5.1 cm, fig. 13(c)) there is clear evidence of six strut-induced pressure disturbances. The disturbances become quite strong at the closest spacing (fig. 13(d)).

Figure 14 shows the blade pressure amplitude spectra corresponding to the average pressures in figure 13. In these spectra the fundamental strut interaction (6/rev.) and its overtones (12/rev. and 18/rev.) are clearly seen at the closer strut spacings. Although weak, there is some evidence of strut interaction at the farthest strut spacing (fig. 14(b)). As expected, with the struts removed (fig. 14(a)) there is no pronounced disturbance at the strut interaction frequencies.

Inflow Control

A major concern of the current study was to evaluate inflow control techniques for simulating flight acoustic performance to determine that the same structures were equally as effective in the anechoic chamber as in the outdoor engine stand. Acoustics tests were performed with the JT15D-1 engine flown on an aircraft, in simulated flight in the NASA Ames 40 x 80 foot wind tunnel, and statically with several inflow control devices. The JT15D fan was likewise tested with two ICD's using the same hardware as was used for the Lewis static engine tests. In the anechoic chamber it was also possible to remove a portion of the inlet boundary layer upstream of the rotor (see fig. 2) in an effort to identify noise associated with boundary layer disturbances or other disturbances near the wall.

Figure 15 compares the sound pressure level spectra obtained with the struts removed for ICD's 5 and 12 at 10 500 rpm fan speed. With the hard duct configuration, figure 15(a), ICD 12 is shown to be somewhat more effective in reducing the BPT level. However, with the 10 percent boundary layer suction in the inlet duct, figure 15(b), both ICD's are shown to essentially reduce the BPT level to that of the surrounding broadband. Thus, it appears that a significant portion of the BPT level generated in static testing originates in the rotor tip region. ICD inlet mating considerations must be a critical element of the overall ICD design, since disturbances originating from this region would tend to enter the rotor in the tip region.

Comparison with JT15D-1 Engine

As was previously discussed, a basic goal of the current program was to validate inflow control structures on the JT15D fan/engine in several test environments. From prior engine tests conducted at Lewis, ICD No. 12 proved to be the most effective in reducting the blade passage tone levels among several ICD designs that were tested.[7] Figure 16 compares results for the Lewis static engine and fan tests using ICD 12. The anechoic chamber data were corrected for distance and bandwidth to the engine measurement conditions. There is reasonably good agreement for the baseline and ICD 12 configurations between the engine and fan. The somewhat more lobed directivity for the fan with inflow control may be caused by the anechoic chamber installation with its greater possibility for wall-induced turbulence (see fig. 2). Boundary layer suction essentially removes these lobes in the directivity results for the fan with ICD 12.

Summary of Results

1. The previously identified interaction between the rotor and the six downstream support struts of the JT15D engine was further investigated through the testing of simulated support struts at three axial spacings. The JT15D fan stage installation in the anechoic chamber did not normally require downstream support struts, allowing the fan stage to also be tested with no struts. The $m = 22$ spinning mode generated by the rotor-strut interaction was evident in the acoustic directivity results, where the sound pressure level was increased by as much as 10 dB at the closest strut spacing. A theoretical prediction for lobe maximum intensity angle based on invariance of the group velocity from duct to far field showed good agreement with the data from these static tests.

2. The quality of the mating region between an ICD and the fan inlet appears to be very important to the overall performance of the ICD in reducing the fan BPT level. By removing residual inlet wall disturbances with boundary layer suction it was possible to further reduce the fan BPT level to that of the surrounding broadband when the support struts were also removed.

3. With the same inflow control device in place, reasonably good agreement was shown between results for the engine on the outdoor test stand and the fan in the anechoic chamber.

References

1. Ho, P. Y., "The Effect of Vane-Frame Design on Rotor-Stator Interaction Noise," AIAA Paper 81-2034, Oct. 1981.

2. Wazyniak, J. A., Shaw, L. M., and Essary, J. D., "Characteristics of an Anechoic Chamber for Fan Noise Testing," NASA TM X-73555, Mar. 1977.

3. McArdle, J. G., Jones, W. L., Heidelberg, L. J., and Homyak, L., "Comparison of Several Inflow Control Devices for Flight Simulation of Fan Tone Noise Using a JT15D-1 Engine," AIAA Paper 80-1025, June 1980.

4. Schoenster, J. A., "Fluctuating Pressures on Fan Blades of a Turbofan Engine," NASA TP-1976, Mar. 1982.

5. Priesser, J. S., Schoenster, J. A., Golub, R. A., and Horne, C., "Unsteady Fan Blade Pressure and Acoustic Radiation from a JT15D-1 Turbofan Engine at Simulated Forward Speed," AIAA Paper 81-0096, Jan. 1981.

6. Chestnutt, D., "Flight Effects of Fan Noise," NASA CP-2242, Sept. 1982.

7. Homyak, L., McArdle, J. G., and Heidelberg, L. J., "A Compact Inflow Control Device for Simulating Flight Fan Noise," AIAA Paper 83-0680, Apr. 1983.

8. Yokoi, S., Nagano, S., and Kakehi, Y., "Reduction of Strut Induced Rotor Blade Vibration with the Modified Stator Setting Angles," International Symposium on Airbreathing Engines, 5th edited by P. A. Paranjpe and M. S. Ramachandra, Bangalore, India, Feb. 1981, pp. 61-1 to 61-7.

9. Kantola, R. A., and Warren, R. E., "Reduction of Rotor-Turbulence Interaction Noise in Static Fan Noise Testing," AIAA Paper 79-0656, Mar. 1979.

10. Englund, D. R., Grant, H. P., and Lanati, G. A., "Measuring Unsteady Pressure on Rotating Compressor Blades," NASA TM-79159, 1979.

11. Heidmann, M. F., Saule, A. V., and McArdle, J. G., "Predicted and Observed Modal Radiation Patterns from JT15D Engine with Inlet Rods," Journal of Aircraft, Vol. 17, No. 7, July 1980, pp. 493-499.

12. Rice, E. J., Heidmann, M. F., and Sofrin, T. G., "Modal Propagation Angles in a Cylindrical Duct with Flow and Their Relation to Sound Radiation," AIAA Paper 79-0183, Jan. 1979.

13. Groeneweg, John F., and Rice, Edward J., "Aircraft Turbofan Noise," ASME Paper 83-GT-197, 28th ASME International Gas Turbine Conference, Phoenix, AZ, Mar. 27-31, 1983.

14. Baumeister, K. J., "Utilizing Numerical Techniques in Turbofan Inlet Acoustic Suppressor Design," NASA TM-82994, Oct. 1982.

TABLE I. - FAN STAGE PARAMETERS AT TAKE-OFF THRUST FOR JT15D-1 ENGINE

Rotor blades		28
Bypass stator vanes		66
Core stator vanes*		71
Speed, rpm		15 740
Rotor diameter, cm (in.)		53 (21)
Bypass ratio		3.3
Bypass pressure ratio		1.5
Total mass flow, kg/sec (lbm/sec)		34.5 (76)
Bypass mass flow, kg/sec (lbm/sec)		26.3 (58)
Bypass rotor-stator spacing	1.83	projected axial
Core rotor-stator spacing	1.42	rotor chords
Rotor-bypass strut spacing	4.92	(5.1 cm)

*Modified from production engine.

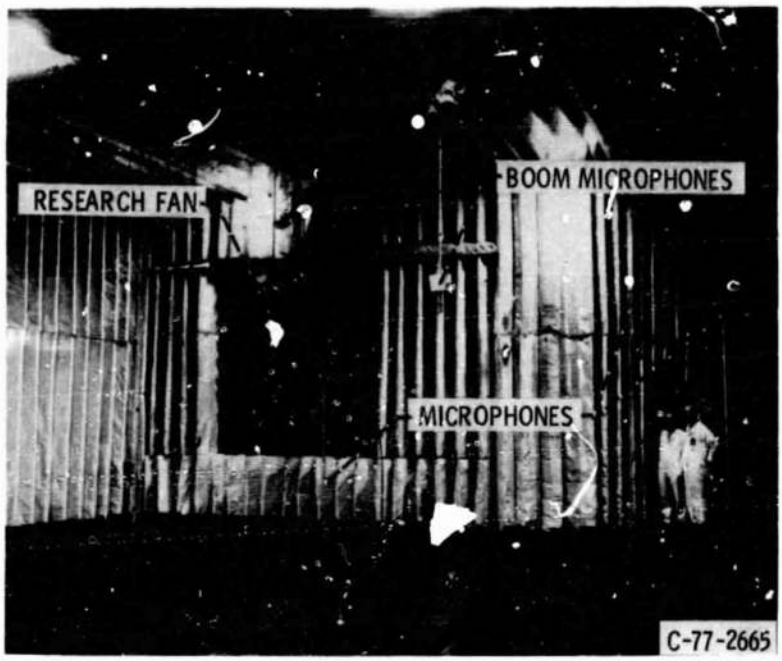

Figure1. - Research fan installed in anechoic chamber.

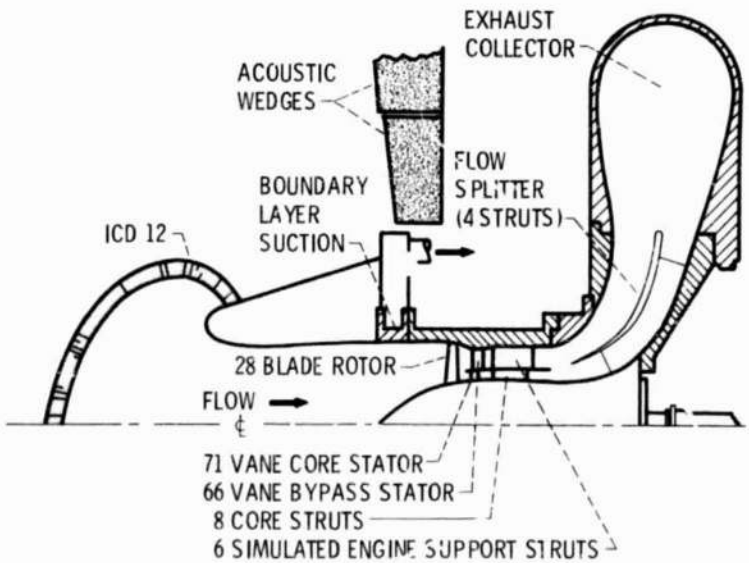

Figure 2. - Sketch of JT15D fan stage installation in Lewis anechoic chamber.

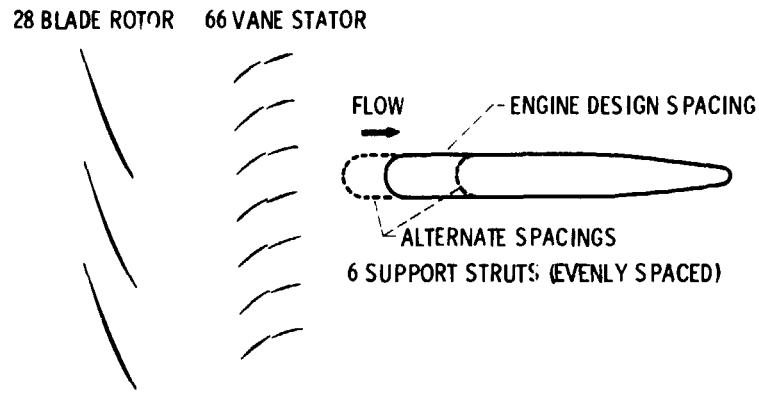

Figure 3. - Unwrapped bypass outside diameter flow passage of the JT15D fan stage showing spacings for the simulated engine support struts.

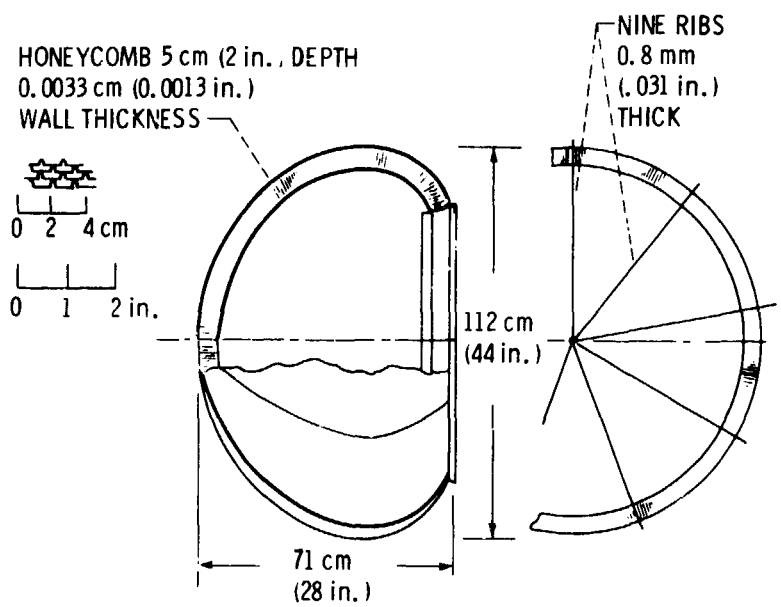

Figure 4. - ICD 12 construction details.

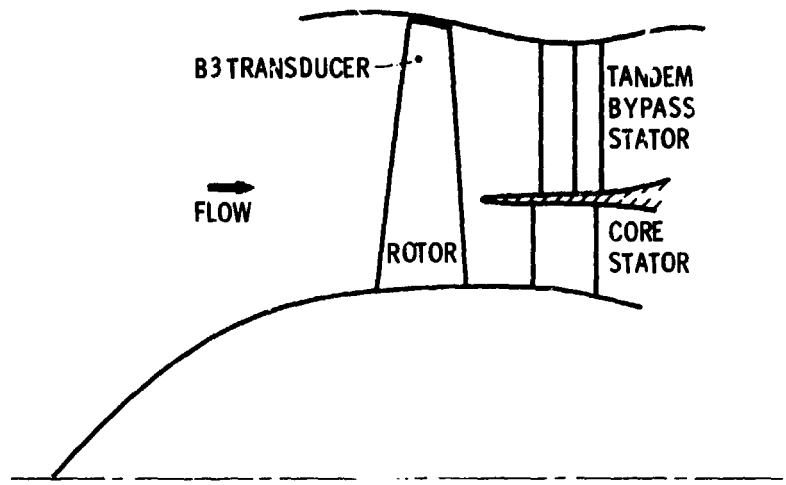

Figure 5. - Location of B3 pressure transducer ("pressure side of blade, 0.38 cm from blade leading edge, 1.90 cm from tip).

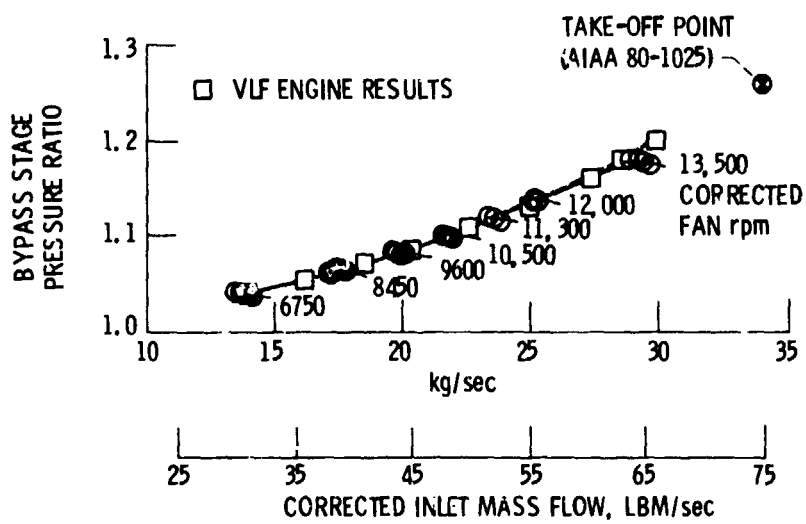

Figure 6. - Fan operating map (VLF engine results shown for comparison).

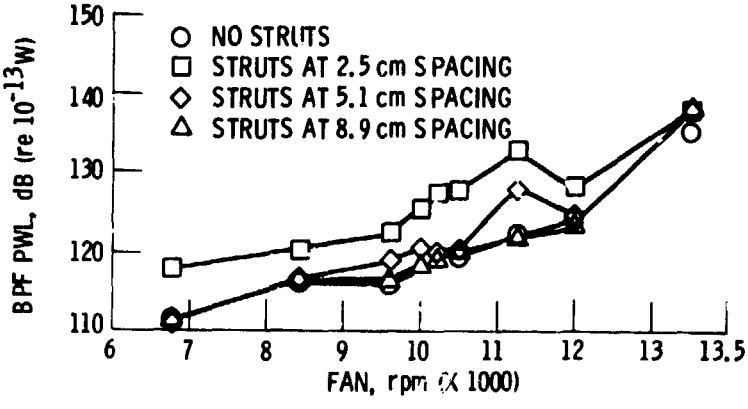

Figure 7. - Strut spacing effect on fundamental blade passage tone power as a function of fan speed (0 - 90°, 80 H_z bandwidth).

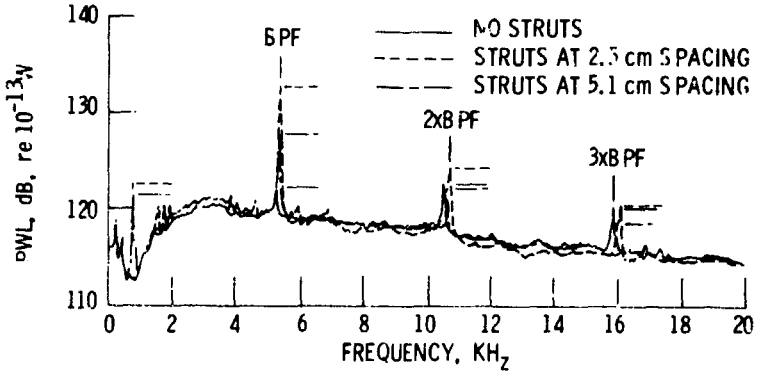

Figure 8. - Sound power level spectra as a function of strut location (0 - 90°, 11,300 rpm, 80 H_z B.W.)

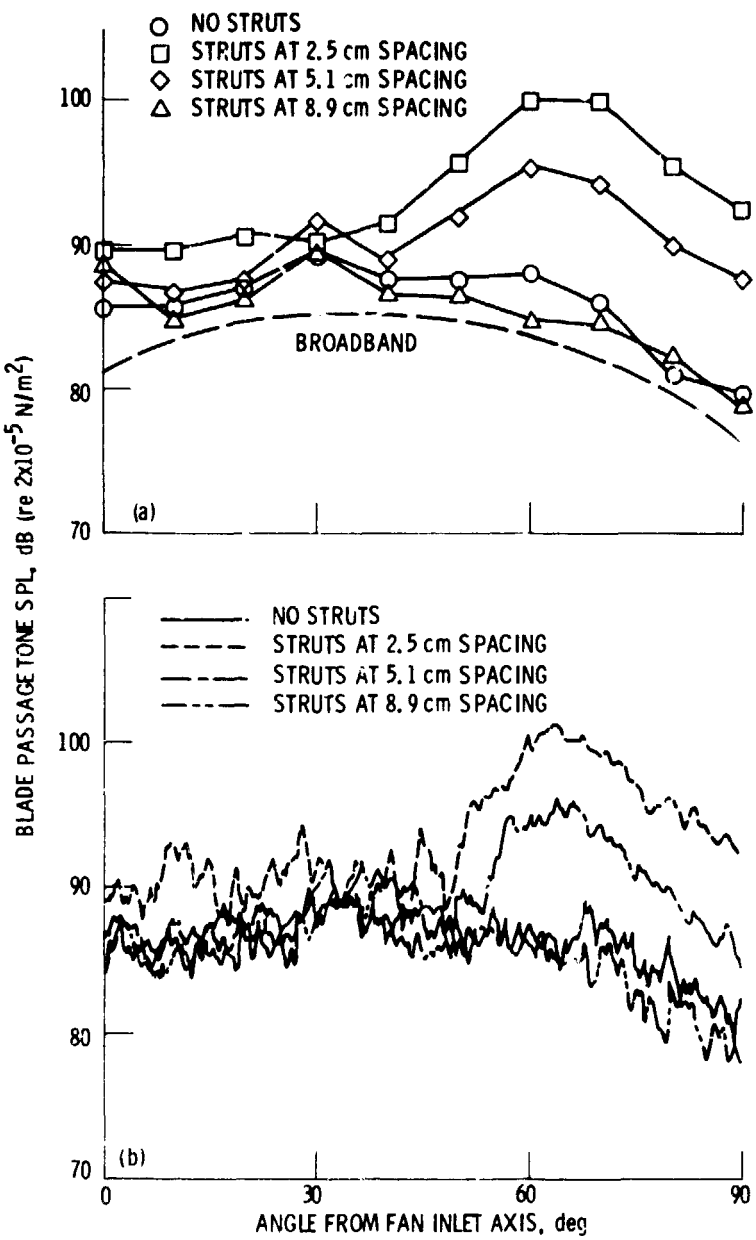

(a) Fixed-position microphones.

(b) Boom microphone.

Figure 9. - Strut spacing effect on blade passage tone directivity (11,300 rpm).

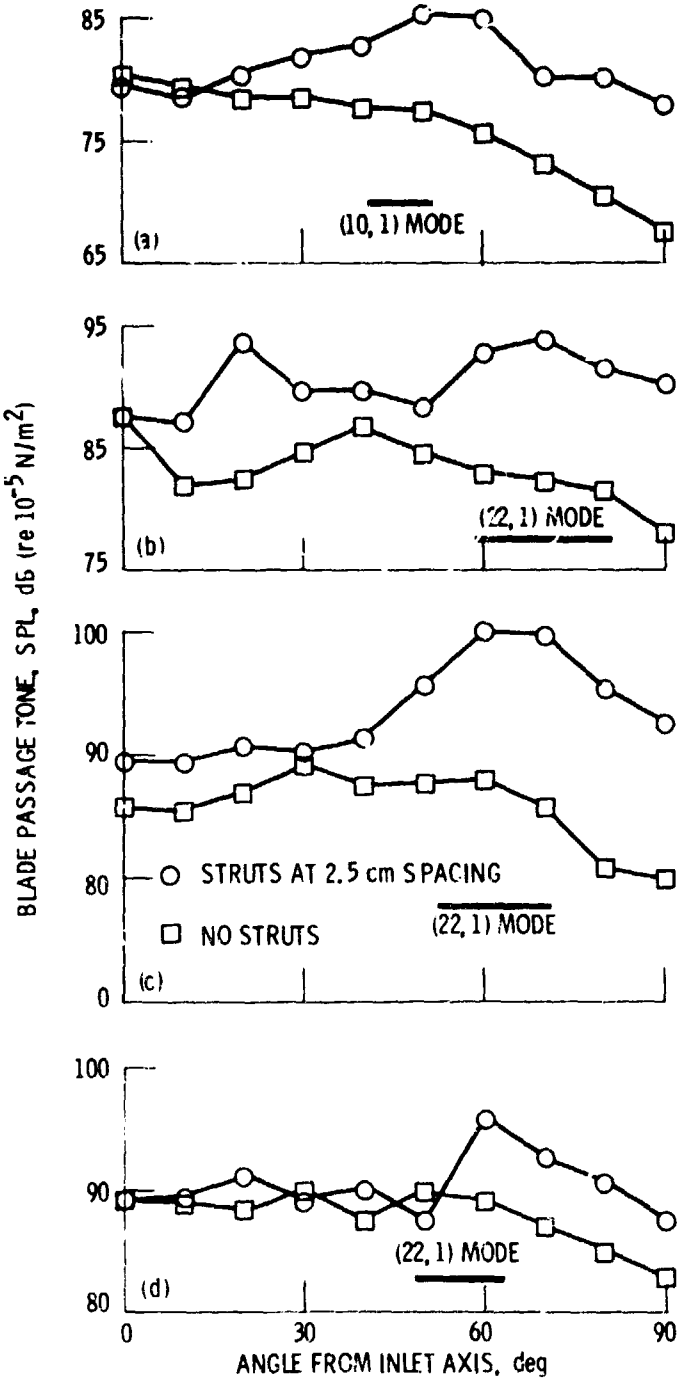

(a) 6750 rpm.

(b) 10, 500 rpm.

(c) 11, 300 rpm.

(d) 12, 000 rpm.

Figure 10. - Blade passage tone directivity at several fan speeds.

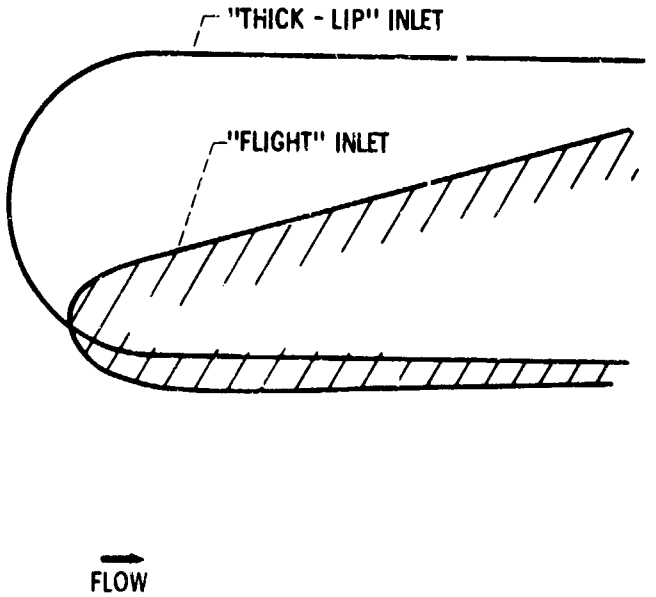

Figure 11. - Comparison of inlet contours for "flight" inlet used in present study and "thick-lip" inlet used in reference 3.

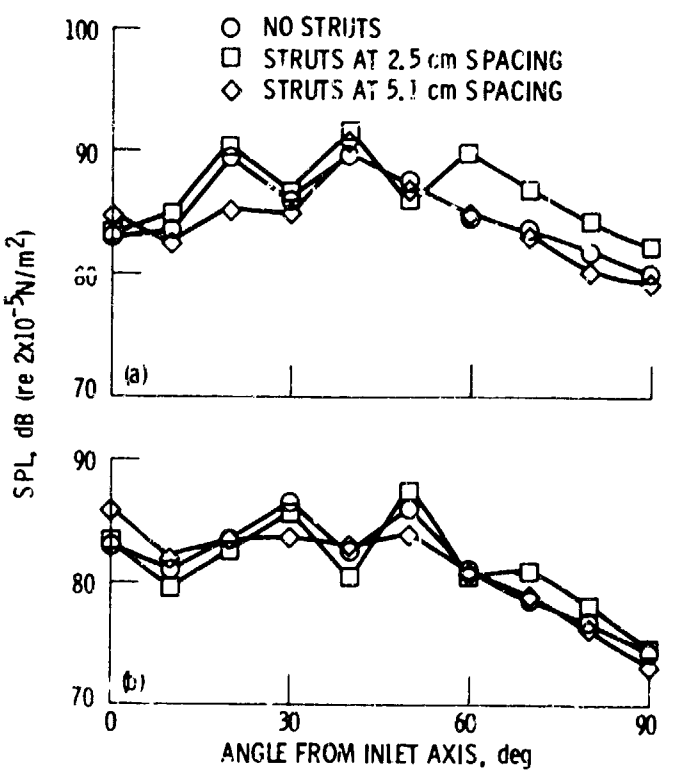

(a) 2 x BPF.

(b) 3 x BPF.

Figure 12. - Strut spacing effect on first and second overtone directivity (11, 300 rpm).

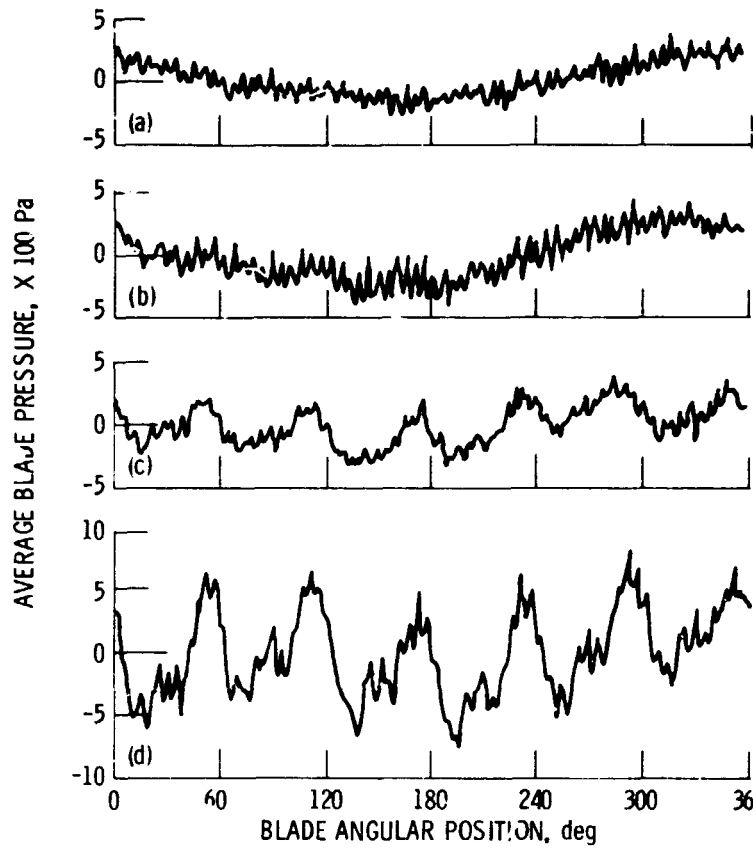

(a) No struts.

(b) Struts at 8.9 cm spacing.

(c) Struts at 5.1 cm spacing (engine location).

(d) Struts at 2.5 cm spacing.

Figure 13. - Average blade pressure as a function of angular position (averaged over 500 revolutions, measured in direction of fan rotation measured from vertical top (12,000 rpm)).

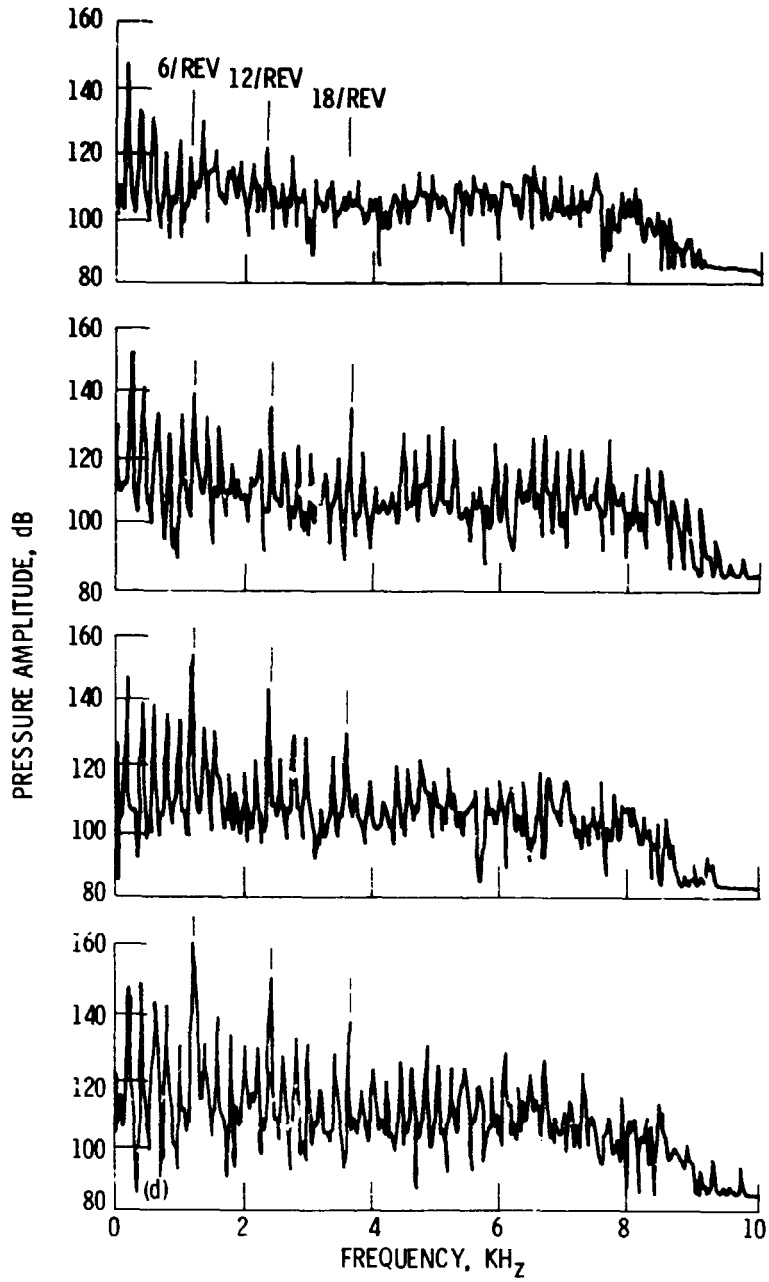

(a) No struts

(b) Struts at 8.9 cm.

(c) Struts at 5.1 cm.

(d) Struts at 2.5 cm.

Figure 14. - Blade pressure amplitude spectra (12,000 rpm; pressure transducer B3).

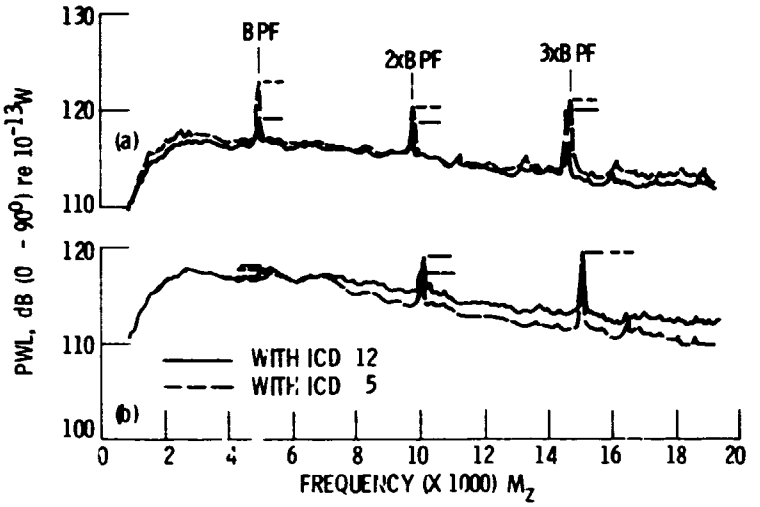

(a) Hard duct.

(b) With B. L. suction.

Figure 15. - Effect of B. L. suction on PWL spectra with support struts removed (10,500 rpm).

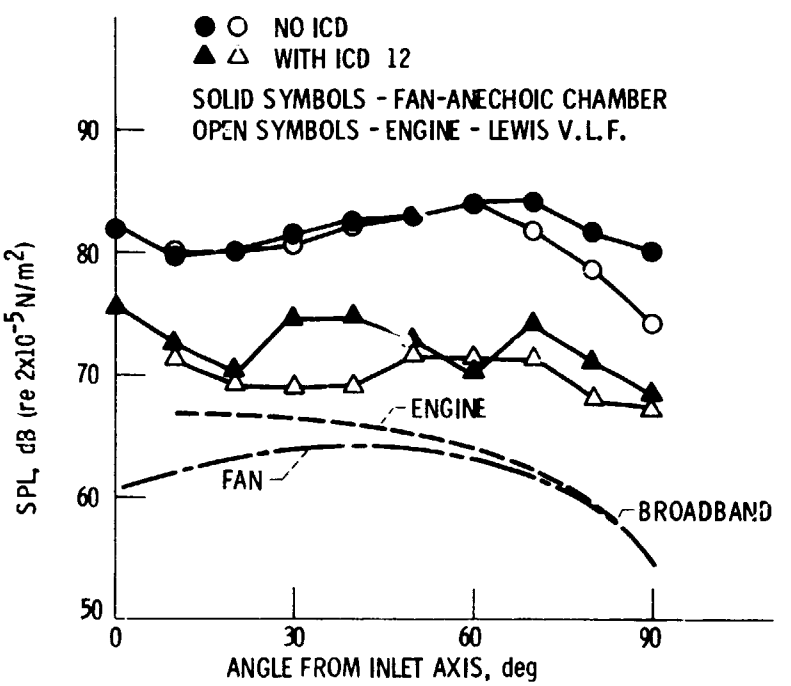

Figure 16. - Blade passage tone directivity (10,500 corrected rpm, results adjusted for 30.5 m (100 ft) radius, 25 m, B. W., fan struts at engine spacing).